

# The nature and dynamics of nonlinear excitations in conducting polymers. Polyacetylene

V I Krinichnyi

## Contents

I. Introduction	81
II. Magnetic parameters of the charge carriers in <i>trans</i> -polyacetylene	83
III. Passage effects and the electronic relaxation of the charge carriers in polyacetylene	86
IV. Dynamics of the soliton and the mechanism of charge transfer in <i>trans</i> -polyacetylene	88
V. Conclusion	91

**Abstract.** The results of studies on various properties of polyacetylene by the high-resolution EPR method in the 2 mm wavelength range are surveyed and treated systematically. The structures and dynamic properties of the paramagnetic centres as well as the mechanism of charge transfer in the neutral polyacetylene are discussed. The bibliography includes 76 references.

## I. Introduction

During recent years, polyacetylene (PA) has attracted considerable attention by investigators because of the uniqueness of its electrodynamic properties, which may prove promising in molecular electronics. Thus when donor or acceptor dopants are introduced, its d.c. conductivity changes by 10–14 orders of magnitude and reaches  $\sigma_{dc} \approx 10^5$ – $10^7$  S m<sup>-1</sup>.<sup>1–3</sup> PA is the simplest conducting polymer in a large class of organic conducting compounds (polyphenylene, polypyrrole, polythiophene, polyaniline, etc.) with similar magnetic and electrodynamic properties; this led to the most vigorous study of these properties in relation to this particular compound.

The *cis*- and *trans*-conformations of PA are distinguished, the latter being thermodynamically more stable.<sup>2,3</sup> The morphology of this polymer depends on the method of synthesis, the structure of the initial monomer, and also on the nature and amount of the dopant introduced. The polymer chains of PA are arranged parallel to one another, forming a fibril several tens of nanometres in diameter and several hundreds of nanometres long. The longitudinal axes of the fibrils are usually randomly oriented in space, but they can be partly or fully oriented during synthesis or by stretching the resulting polymer. The polymer chains in such fibrils are close-packed. The PA crystal lattice has the following parameters:  $a = 0.761$  nm,  $b = 0.439$  nm, and  $c = 0.447$  nm (*cis*-PA) and  $a = 0.424$  nm,  $b = 0.732$  nm, and  $c = 0.246$  nm (*trans*-PA).<sup>4,5</sup>

In each monomer unit of PA, three out of four valence electrons are in the hybridised  $sp^2$  orbitals: two electrons

participate in the formation of two  $\sigma$ -bonds responsible for the formation of the quasi-one-dimensional (1D) lattice, while the third is involved in the formation of a bond with a hydrogen atom. The last valence electron is in the  $2p_z$  orbital oriented at right angles to the plane in which the remaining three electrons are located. Thus the  $\sigma$ -bonds form a low-lying completely filled valence band, while the  $\pi$ -bonds of the monomer units form a partly filled conduction band. If the lengths of all the C–C bonds were equal, then undoped *trans*-PA could be regarded as a 1D-metal with a half-filled conduction band. In reality, the system represents a set of monomeric CH groups linked by alternating double and longer single bonds, which execute longitudinal vibrations. Such a system is unstable (Peierls instability) and the alternation in it takes place almost without energy expenditure. Calculation has shown<sup>6</sup> that the degeneracy of the system leads to the generation on the *trans*-PA chains (with an energy expenditure of 0.42 eV) of nonlinear topological excitations — solitons — with a spin  $s = \frac{1}{2}$ , an effective number of C–C bonds  $N \approx 15$ , an effective mass  $m_s^*$  equal to six times the free electron masses  $m_e$ , and a high 1D-mobility. The energy level of the solitons is located at the centre of the energy gap of the polymer. This phenomenon determines to a large extent the fundamental properties of *trans*-PA, including the relatively large width of the energy gap, which is  $\sim 1.4$  eV. Some experiments (see, for example, Refs 7–9) yield the effective number of C–C bonds  $N \approx 50$  and  $m_s^* = (0.15 - 0.40)m_e$ .

The spin-charge conversion is characteristic of a single soliton in *trans*-PA: the neutral soliton corresponds to a radical with a spin  $s = \frac{1}{2}$ , whereas a negatively or positively charged soliton lacks spin and becomes diamagnetic. Therefore, in n-type doping, the energy level of the soliton becomes fully occupied, whilst in p-type doping it becomes entirely unoccupied. For a low level of doping, only some of the neutral solitons become charged. With increase in the level of doping, all the solitons become diamagnetic and their individual energy levels merge into the soliton band located in the middle of the energy gap of the polymer. The formation of the soliton band leads to charge transfer by the spin-free carriers after the semiconductor–metal transition. This conduction mechanism, which includes the motion of charged solitons in an occupied or unoccupied band, differs significantly from the charge transfer process in classical semiconductors.

In PA, there is the possibility of the occurrence of various charge transfer processes, which may be arranged in the following sequence in order of their decreasing probability: 1D-conduction along polymer chains; charge transfer in hops between polymer chains; tunnelling of the charge between highly conducting

V I Krinichnyi Laboratory for the Synthesis of Electrically Conducting Compounds, Institute of Chemical Physics in Chernogolovka, 142432 Chernogolovka, Moscow Region, Russian Federation  
Fax (7-096) 515 35 88. Tel. (7-096) 524 50 35

Received 6 July 1995

*Uspekhi Khimii* 65 (1) 84–96 (1996); translated by A K Grzybowski

domains of fibrils separated by regions with a lower conductivity; or fluctuation-induced tunnelling of the charge between fibrils.

It is entirely evident that the contribution of each of these processes depends on the properties of the initial polymer and may change during its doping.

Conjugated polymers are characterised by the presence of a  $\pi$ -electron system and a partly filled band structure, which determines important electronic properties of these systems. In contrast to the classical semiconductors, apart from the activated electron transport,<sup>10</sup> in PA there is also the possibility of phonon-assisted charge tunnelling between the energy levels of solitons<sup>11</sup> and of variable range hopping conductivity (VRH)<sup>12</sup> characterised by different frequency and temperature dependences  $\sigma(\nu_e, T)$ . Such diversity of electron transport is associated with the generation of nonlinear soliton-type excitations and may be associated directly with the evolution of both the crystalline and the electronic structures of the system.

Several theoretical approaches have been put forward for the description of the mobility of the soliton in *trans*-PA. They were developed in terms of the concept of the Brownian 1D-diffusion of solitons interacting with the lattice phonons<sup>13</sup> and of the scattering of solitons by optical and acoustic phonons in *trans*-PA.<sup>14</sup> One of them predicts a quadratic dependence of the frequency of the 1D-diffusion  $\nu_{1D} = D_{1D}c_1^{-2}$  ( $D_{1D}$  is the 1D-diffusion coefficient and  $c_1$  is the length of the soliton jump along the polymer chain) on temperature. In the second case, the dependences have the form  $\nu_{1D}(T) \sim T^{-1/2}$  and  $\nu_{1D}(T) \sim T^{1/2}$  for the optical and acoustic phonons respectively. Calculations showed<sup>15</sup> that the frequency of the 1D-diffusion of the soliton should not exceed the limiting value  $\nu_{1D}^F = 3.8 \times 10^{15}$  Hz near the Fermi level.

Many fundamental properties of PA and other conjugated polymers are determined by the existence in them of the localised paramagnetic centres (PC) and/or such centres delocalised along the polymer chains, so that the majority of the investigations of these compounds have been carried out by the EPR method.<sup>16,17</sup> We shall consider certain possibilities for the study of PA by this method.

At relatively low measuring frequencies ( $\nu_e \leq 10$  GHz), PA gives rise, like the classical  $\pi$  electron systems, to a single symmetrical EPR line with  $g = 2.002634 \pm 0.000015 \approx g_e$ .<sup>18</sup> The  $g$ -factor deviates from  $g_e$  mainly owing to some contribution by the orbital angular momentum of the unpaired electron to its overall magnetic moment. The EPR line consists of a superposition of individual weakly resolved lines corresponding to the hyperfine interaction of the spin with the carbon nuclei on which the soliton is localised.

According to the model proposed by Su et al.,<sup>6</sup> the defect-free undoped *cis*-PA contains no paramagnetic centres and should therefore be diamagnetic. In reality, *cis*-PA contains 5%–10% of short segments of *trans*-PA, mainly at the ends of the chains.<sup>3,16</sup> where the trapping of solitons is most likely.<sup>19</sup> Such an isomer therefore gives rise to a relatively weak broad EPR line, in which the distance between the peaks is  $\Delta B_{pp} = 0.6 - 1.0$  mT ( $g = 2.002634$ ) and the hyperfine interaction tensor constants are  $A_{xx} = -1.16$  mT,  $A_{yy} = -3.46$  mT, and  $A_{zz} = -2.32$  mT<sup>20</sup> (the  $x$ ,  $y$ , and  $z$  axes are directed along the crystallographic  $a$ ,  $c$ , and  $b$  axes respectively). On thermal *cis*–*trans* isomerisation, the concentration of paramagnetic centres increases from  $N \sim 10^{18}$  spins  $g^{-1}$  (this is equivalent to one spin per  $\sim 44000$  CH groups) in *cis*-PA to  $N \sim 10^{19}$  spins  $g^{-1}$  (or one spin per 3000–7000 CH groups) in *trans*-PA.<sup>21</sup> This is accompanied by a sharp narrowing of the line of 0.03–0.50 mT.<sup>16,22</sup> The latter quantity depends on the average length of the *trans*-sections and represents a linear function of the concentration of the  $sp^3$ -defects.<sup>23</sup> A dependence of the type  $\Delta B_{pp} \sim Z^{2.3}$  has been obtained for PA doped with metal ions having an atomic number  $Z$ .<sup>24</sup> The line width of *trans*-PA partially ordered by stretching proved sensitive to the direction of stretching  $c$  of the specimen in a magnetic field with a strength

$B_0$ .<sup>23,25–28</sup> Thus, in the case of the parallel direction of the external magnetic field strength vector relative to the  $c$  axis, the line width is 0.48 mT, whilst in the case of the perpendicular direction it is 0.33 mT.<sup>23</sup>

The EPR spectrum of *trans*-PA may be represented by a superposition of the contributions of the trapped and highly mobile solitons with concentrations  $n_1$  and  $n_2$  respectively, the ratio of which varies with temperature, and also of the contributions due to other fixed centres, the appearance of which is associated with the presence of traces of catalyst and/or oxygen molecules. In  $n$ - and  $p$ -doping, the concentration of paramagnetic centres in *trans*-PA changes monotonically for a virtually constant  $g$ -factor,<sup>16,17</sup> which indicates the retention of the nature of the paramagnetic centres responsible for the EPR signal.

Numerous studies on the paramagnetic susceptibility  $\chi$  of neutral PA have shown<sup>17</sup> that both its conformers exhibit Curie paramagnetism ( $\chi \sim T^{-1}$ ) at  $T \leq 300$  K, whereas, according to the data of Tomkiewicz et al.,<sup>29</sup> the magnetic susceptibility of *cis*-PA does not obey the Curie law in the temperature range 4–300 K. The reasons for this discrepancy are so far obscure.

High-frequency magnetic field modulation as well as electron spin-echo have been used to investigate the interaction of the unpaired electron with other electrons or with the *trans*-PA lattice. Since a neutral soliton has an electron spin interacting with the spins of the hydrogen nuclei, its dynamics may be investigated by complementary NMR and EPR methods.

The quasi-one-dimensional mobility of the soliton has been investigated by NMR within the framework of the Brownian 1D-diffusion of the soliton.<sup>30,31</sup> The dependence of the nuclear spin–lattice relaxation time  $\tau_1$  on the precession frequency of the nuclear spin  $\tau_1 \sim \nu_p^{1/2}$ , obtained for undoped and doped *trans*-PA specimens, corresponded to the characteristic spectrum of the spin 1D-diffusion. The frequency of the 1D-diffusion of the soliton in undoped *trans*-PA proved to be  $6 \times 10^{14}$  Hz (at room temperature) and showed a quadratic temperature dependence. Estimates showed<sup>30</sup> that the rate of diffusion may increase by more than three orders of magnitude following the introduction of various dopants into the polymer.

However, it must be emphasised that the motion of the soliton influences only indirectly the nuclear spin relaxation time. Since the interaction of the diffusing proton with a fixed electron spin is also characterised by the frequency dependence  $\tau_1 \sim \nu_p^{1/2}$ ,<sup>32</sup> this can lead to an incorrect interpretation of the results obtained by NMR spectroscopy. Thus, on the basis of the kinetics of the decay of the <sup>13</sup>C NMR signal, it has been concluded<sup>33</sup> that there are no mobile unpaired electrons at all in *trans*-PA. However, according to Ziliox et al.,<sup>34</sup> this conclusion may be valid only for the specific specimens investigated by Masin et al.<sup>33</sup>

The EPR spectroscopic method is a priori more effective in the study of the dynamics of the soliton in *trans*-PA, since the electronic relaxation times are unambiguously related to the diffusion of the soliton.

The spin dynamics in *trans*-PA has been investigated with the aid of low-frequency steady-state EPR<sup>26–28,35,36</sup> and the spin-echo method.<sup>37–39</sup> The relations  $\tau_{1,2} \sim \nu_e^{1/2}$  and  $\nu_{1D}(T) \sim T^2$  ( $\tau_1$  and  $\tau_2$  are the spin–lattice and spin–spin relaxation times) were obtained by the first method in the frequency range  $\nu_e = 5 - 450$  MHz. They indicate the 1D-diffusional spin motion in *trans*-PA with  $\nu_{1D} \geq 10^{13}$  Hz and the anisotropy  $\nu_{1D}/\nu_{3D} = 10^6 - 10^7$  (at room temperature). A similar frequency dependence of the rate of diffusion has been observed also at higher recording frequencies  $\nu_e = 9 - 14$  GHz.<sup>38,40</sup> However, the spin diffusion frequency determined by the spin-echo method is  $\nu_{1D} \leq 10^{11}$  Hz (at room temperature) and exhibits a more complex temperature dependence.<sup>37</sup>

Thus the data obtained by different methods and by different investigators concerning the dynamics of solitons in *trans*-PA are extremely contradictory and do not always find an unambiguous interpretation. EPR spectroscopy is the most promising method

for the investigation of the composition and dynamics of the paramagnetic centres. However, it suffers from considerable limitations owing to the low spectral resolution and the high spin-spin exchange at  $\nu_e \leq 40$  GHz. This prevents the separate recording in *trans*-PA of localised and mobile  $\pi$ -radicals with similar magnetic parameters.<sup>22</sup>

It had been shown earlier in relation to certain organic radicals<sup>41,42</sup> that in the 2 mm wavelength range there is a significant increase in the accuracy and the information content of the EPR method in the study of the structure and molecular dynamics of radicals with  $g \approx g_e$  in model systems and biological polymers. The high resolving power of the method, attained in this frequency range, converts the  $g$ -factor of organic free radicals into an important information parameter. This makes it possible to discover the anisotropic character of the slow molecular motions, to extend the range of the measured correlation times for the rotation of the radical, and also to identify the structure of the radical and of its microenvironment.

The high spectral resolution of the EPR method in the 2 mm range yields important information about the spin and molecular dynamics in organic conducting compounds.<sup>43</sup> The present review is devoted to the consideration of the experimental data obtained in the study of the structure and electrodynamic properties of PA by two-millimetre EPR spectroscopy. The theoretical foundations of the method have been described in fair detail in a number of monographs† and will not therefore be considered here.

## II. Magnetic parameters of the charge carriers in *trans*-polyacetylene

For a more correct determination of the magnetic resonance parameters of the paramagnetic centres in PA, various films of *cis*- and *trans*-PA were investigated over a wide EPR frequency range.<sup>44</sup>

In the 3 cm EPR range ( $\nu_e = 9.8$  GHz), the *cis*- and *trans*-PA specimens are characterised by a single symmetrical line with  $g = 2.0026$  and the width between the peaks  $\Delta B_{pp} = 0.67$  mT (*cis*-PA) and 0.22 mT (*trans*-PA) (Fig. 1). The latter quantity exceeds the minimum width of the *trans*-PA spectral line,<sup>16</sup> and is apparently associated with the presence in the specimen of oxygen molecules or shorter  $\pi$ -conjugated chains, but is within the limits of the variation of the  $\Delta B_{pp}$  obtained for different *trans*-PA specimens.<sup>22</sup> This line is broadened by 0.05–0.17 mT at 77 K, probably as a consequence of the decrease in the frequency of the librations of the polymer chains and is additionally broadened by 0.1 mT when the polymer comes into contact with atmospheric oxygen, apparently owing to the strengthening of the trapping of the mobile solitons in *trans*-PA.<sup>45</sup>

An increase in the recording frequency to 37.5 GHz results in a slight increase in the width of the lines in the PA spectrum (Table 1) with retention of the symmetry.

In the 3 mm EPR range, the line width of the *cis*-PA spectrum increases to 0.84 mT. This is accompanied by an additional broadening of the high-field spectral peak owing to the manifestation of the anisotropy of the  $g$ -factor. *trans*-PA is characterised by a line with  $g = 2.00270$ ,  $\Delta B_{pp} = 0.37$  mT, and the asymmetry factor  $A:B = 1.1$  (the ratio of the amplitudes of the high-field and low-field spectral peaks).

† J D Memory *Quantum Theory of Magnetic Resonance Parameters* (McGraw-Hill, New York, 1968)

B Ranby, J F Rabek *EPR Spectroscopy in Polymer Research* (Springer, Berlin, 1977)

C P Slichter *Principles of Magnetic Resonance* 2nd Ed. (Springer, Berlin, 1978)

*Theoretical Foundations of Electron Spin Resonance* Ed. J E Harriman (Academic Press, New York, 1978)

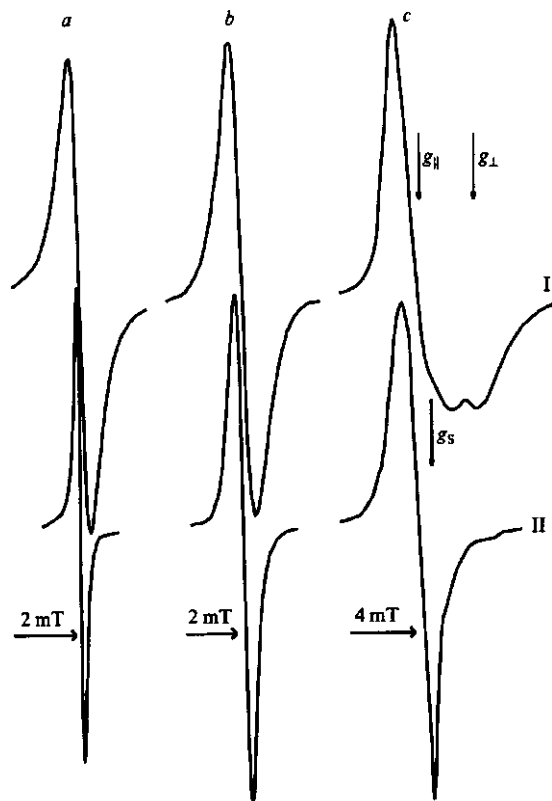


Figure 1. EPR spectra of *cis*-(I) and *trans*-polyacetylene (II) recorded in the 3 cm (a), 2 mm (b), and 0.6 mm (c) ranges at room temperature under an inert atmosphere. The positions of the components of the  $g$ -tensor of the localised solitons ( $g_{\parallel}$  and  $g_{\perp}$ ) and the  $g_s$ -factor of the delocalised solitons are indicated.

Table 1. The line widths (in mT) and the distances between the spin packets (in Hz) for the paramagnetic centres in neutral polyacetylene at different recording frequencies at 300 K.

$\nu_e$ /GHz	$\Delta B_{pp}^i$		$\Delta B_{pp}$	$\Delta\omega_{ij} \times 10^8$		
	I	II		I	II	III
9.8	0.70	0.25	0.06 <sup>a</sup>	1.7	1.0	0.8 <sup>a</sup>
37.5	0.75	0.30	0.11 <sup>a</sup>	1.8	1.2	1.3 <sup>a</sup>
94.3	0.85	0.45	0.18	1.9	1.4	1.7
139	0.95	0.61	0.30	2.3	2.2	2.2
250	1.82	1.60	0.50	2.8	2.8	2.9
349	2.42	2.52	0.62	3.2	3.5	3.2
428	2.53	1.91	0.81	3.3	3.1	3.7

Remarks. I—solitons localised in *cis*-PA; II—solitons localised in *trans*-PA; III—solitons delocalised in *trans*-PA.

<sup>a</sup> Values obtained by extrapolation.

In the 2 mm range for the recording of the EPR spectrum, there is a further increase in  $\Delta B_{pp}$  to 1.1 mT (in *cis*-PA) and 0.5 mT (in *trans*-PA) accompanied by a more marked manifestation of the anisotropy of the  $g$ -factor in *cis*-PA and a greater asymmetry of the spectral line ( $A:B = 1.3$ ) in *trans*-PA (Fig. 1).

In order to elucidate the possible dependence of the PA spectral line width on the orientation of the magnetic field, a study has been made<sup>46</sup> of partly oriented *cis*- and *trans*-PA specimens. The investigation showed that the line width in the spectrum of the initial *cis*-PA specimen increases after slight stretching of the film from 1.23 to 1.45 mT ( $T = 300$  K).

The magnetic parameters of the partly oriented *cis*-PA did not change significantly on varying the angle between the directions of stretching and the external magnetic field, whereas the line width in *trans*-PA changed nonmonotonically from 0.60 to 0.68 mT at room temperature.

With increase in the recording frequency, a further broadening and a further increase in the asymmetry of the EPR spectral lines of both conformers were observed (Fig. 1). Analysis carried out by the method described by Lebedev and Muromtsev<sup>47</sup> showed that the spectrum of *cis*-PA, presented in Fig. 1, may be assigned to paramagnetic centres with the *g*-tensor components  $g_{\parallel} = 2.00283(5)$  and  $g_{\perp} = 2.00236(5)$  ( $g_{\parallel}$  and  $g_{\perp}$  correspond to the parallel and perpendicular directions of the external magnetic field relative to the crystallographic *c* axis of the polymer chain). The values of the *g*-tensor quoted exceed somewhat the values of  $g_{\parallel}$  and  $g_{\perp}$  determined experimentally<sup>48</sup> but are close to  $g_{\parallel} = 2.0034$  and  $g_{\perp} = 2.0028$  calculated in the same study for localised paramagnetic centres. The quantity  $g_{\parallel}$  differs from  $g_e$  by  $\Delta g = 5 \times 10^{-4}$ . This deviation corresponds to the excitation of the electron from the bonding  $\sigma_{C-C}$  orbital to the antibonding  $\pi^*$  orbital with  $\Delta E_{\sigma\pi^*} = 2\lambda_c \Delta g^{-1} = 14.4$  eV (here  $\lambda_c = 3.6$  meV is the constant for the spin-orbital interaction of the unpaired electron with the nucleus of the carbon atom), which is close to the corresponding value calculated for the C-C bond in  $\pi$ -conjugated systems.<sup>49</sup> Other electronic transitions with a greater  $\Delta E_{ij}$  do not contribute significantly to  $\Delta g$ . Thus the line form in the *cis*-PA spectrum as well as the agreement between the experimental and theoretical values of  $\Delta E_{\sigma\pi^*}$  indicate the existence of localised paramagnetic centres in this isomer.

The transformation of the line shape on *cis-trans* isomerisation of PA evidently indicates the appearance in the PA of mobile paramagnetic centres with  $g_s = 2.00268$  (Fig. 1) during the occurrence of this process. The similarity of the isotropic *g*-factor of the localised paramagnetic centres [ $\langle g \rangle = \frac{1}{3}(g_{\perp} + 2g_{\parallel}) = 2.00267$ ] and the *g*-factor of the delocalised paramagnetic centres indicates the virtually complete averaging of the components of the *g*-tensor of the mobile paramagnetic centres owing to their 1D-diffusion at a minimal rate.<sup>50</sup>

$$v_{1D}^0 \geq \frac{1}{h}(g_{\parallel} - g_{\perp})\mu_B B_0 \quad (1)$$

Computer simulation<sup>44</sup> confirmed this hypothesis. A similar averaging of the components of the anisotropic *g*-factor was recorded by ourselves also on 'unfreezing' the 1D-diffusion of polarons in other organic conducting polymers.<sup>43</sup> Thus two types of paramagnetic centres exist in undoped *trans*-PA, namely the neutral soliton trapped at the ends and/or on short segments of the  $\pi$ -conjugated chain<sup>19</sup> and the soliton moving along the polymer chain with a frequency  $v_{1D}^0 > 2 \times 10^8$  Hz. The value of  $v_{1D}^0$  obtained is significantly less than the lower limit of the rate of diffusion of solitons previously predicted.<sup>30</sup> The concentrations of the corresponding paramagnetic centres are  $n_1 = 1.1 \times 10^{-3}$  and  $n_2 = 6 \times 10^{-5}$  spins per carbon atom. It is necessary to note that the latter quantity is almost two orders of magnitude smaller than the value predicted previously.<sup>18,51</sup>

Analysis of the form of the spectra of *cis*- and *trans*-PA specimens by the method of Tikhomirova and by Voevodskii<sup>52</sup> showed that, for  $\nu_e \geq 140$  GHz, the distribution of the individual spin packets in their low-field sections is described by Lorentzian (at the centre) and Gaussian (on the wings) functions. On the other hand, the high-field parts of the spectra are characterised by a Lorentzian distribution of the spin packets. This made it possible to calculate the frequencies of the spin-spin exchange  $\nu_{ex}$  between the localised paramagnetic centres in *cis*- and *trans*-PA, which are  $3 \times 10^7$  and  $1.2 \times 10^8$  Hz respectively. These quantities are consistent with  $\nu_{ex} \geq 10^7$  Hz obtained for *trans*-PA.<sup>22</sup> Thus, at a recording frequency  $\nu_e \geq 16$  GHz, the distance between the spin packets  $\Delta\omega_{ij}$  exceeds  $\nu_{ex}$ , so that the spin packets may be regarded as virtually noninteracting and the

width of the lines of the localised paramagnetic centres is described by the equation<sup>53</sup>

$$\Delta B_{PP} = \Delta B_{PP}^0 + \frac{\Delta\omega_{ij}^2}{8\nu_{ex}}, \quad (2)$$

where  $\Delta B_{PP}^0$  is the line width in the absence of interaction between the paramagnetic centres. Assuming that the relaxation time  $\tau_2^{\text{mob}}$  of the delocalised paramagnetic centres is  $1.8 \times 10^{-7}$  s for *trans*-PA at room temperature<sup>54</sup> and taking into account the strong interaction between solitons with different mobilities, it is possible to calculate the line width in the spectrum of the mobile soliton  $\Delta B_{PP}$ , which proved to be 32  $\mu$ T. This quantity agrees well with the line width in the spectrum of the mobile soliton (12–38  $\mu$ T) predicted by Holczer et al.<sup>22</sup>

The values of  $\Delta\omega_{ij}$  calculated for the paramagnetic centres in *cis*- and *trans*-PA by Eqn (2) are presented in Table 1. The table shows that the isomerisation of PA is accompanied by a decrease in  $\Delta\omega_{ij}$  for the paramagnetic centres in both conformers. Taking into account the increase in  $\nu_{ex}$  indicated above, one may conclude that the change of precisely these quantities is the cause of the sharp narrowing of the EPR spectra (for  $\nu_e \leq 10^{10}$  Hz) during the *cis-trans* isomerisation of PA. This conflicts with the view current up to the present time that the line narrowing indicated above is possible only by virtue of the 'unfreezing' of the 1D-diffusion of most of the solitons in *trans*-PA.<sup>13,16,30</sup>

The dependences of the broadening of the lines of the localised and mobile paramagnetic centres on the measuring frequency are illustrated in Fig. 2. The latter shows that the line width in the spectrum of the paramagnetic centres localised in both conformers varies almost quadratically with  $\nu_e$ , in conformity with Eqn (2), which constitutes additional evidence for the weak interaction of the spin packets in PA. On the other hand, the line width in the spectrum of the delocalised paramagnetic centres increases in accordance with the law  $\Delta B_{PP}^{\text{mob}} \sim \nu_e^{3/2}$ , which is a consequence of the stronger spin-phonon interaction in *trans*-PA owing to the 1D-motion of the solitons.

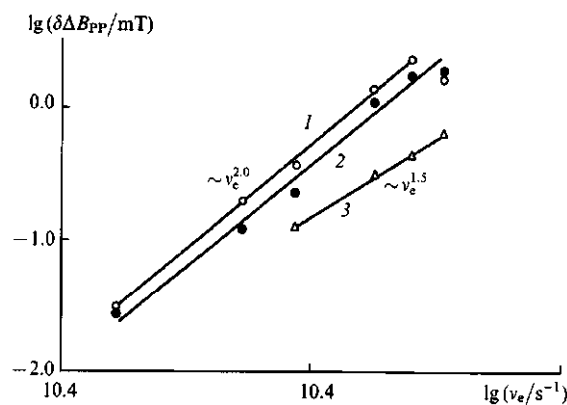


Figure 2. Logarithmic dependences of the broadening ( $\delta B_{PP}$ ) of the EPR lines of the paramagnetic centres localised in *trans*-polyacetylene (line 1) and *cis*-polyacetylene (line 2) (relative to the quantity  $\Delta B_{PP}^0$  measured at 9.8 GHz), as well as the paramagnetic centres delocalised in *trans*-polyacetylene (line 3) (relative to the quantity  $\Delta B_{PP}^0$  measured at 94.3 GHz) on the recording frequency at room temperature.

It is seen from the analysis of Table 1 that, at least for  $\nu_e \leq 140$  GHz, the following familiar relation holds:<sup>55</sup>

$$(\Delta B_{PP}^{\text{mob}})^3 = \frac{\gamma_e (\Delta B_{\perp}^{\text{loc}})^4}{v_{1D}}, \quad (3)$$

where  $\gamma_e$  is the gyromagnetic ratio for the electron. This follows from the theory of random motion and characterises the line narrowing in the EPR spectrum of a semiconductor when spin 1D-diffusion arises in the latter with an effective rate  $\nu'_{1D} \approx 2 \times 10^{11}$  Hz.<sup>56</sup> We may note that another relation is valid for spin 3D-motion:

$$\Delta B_{PP}^{\text{mob}} = \frac{\gamma_e (\Delta B_1^{\text{loc}})^2}{\nu'_{1D}}$$

This constitutes additional evidence for the 1D-diffusion of solitons in *trans*-PA. For  $\nu_e > 140$  GHz, Eqn (3) does not hold, apparently owing to the similarity of the quantities  $\nu_e$  and  $\nu'_{1D}$ .

Fig. 3a presents the temperature dependences of the reduced concentrations of the paramagnetic centres ( $N$ ) of certain *cis*-PA specimens, which can be fitted by the following function:

$$N(T) = A \exp\left(-\frac{E_a}{kT}\right) + BT^{-n} \quad (1 \leq n \leq 2), \quad (4)$$

where  $A$  and  $B$  are constants and  $E_a$  is the activation energy. The first term of Eqn (4) is determined by the librations of the polymer chains, the activation energies of which for different specimens are 0.035–0.055 eV. A similar manifestation of the electron–phonon interaction (mainly in the form of fluctuations of the electronic polarisation energy of the order of several millielectron volts) has been observed in organic crystalline semiconductors.<sup>57</sup> As can be seen from the figure, the activated ordering of the magnetic moments of the spins makes the main contribution to the paramagnetic susceptibility only at high temperatures. In the range of temperatures below a critical temperature  $T_c \approx 150$  K, this process competes with others, in particular with the process described by the Curie equation ( $n = 1$ ). The contributions of the processes involving the orientation of the magnetic moments of the unpaired electrons are different for different *cis*-PA specimens.

The concentration of the paramagnetic centres in the *trans*-PA specimens is also characterised by an anomalous temperature dependence (Fig. 3b). As in the case of *cis*-PA, the main contribution to the paramagnetic susceptibility of *trans*-PA in the high-temperature region comes from the first term of Eqn (4). The increased value of  $E_a$  ( $E_a = 0.06 - 0.19$  eV) may be explained by the increase in the rigidity of the polymer chains and in their packing density on *cis*–*trans* isomerisation. This is apparently

also the cause of the shift of the critical temperature into the region  $T_c \approx 250$  K.

In contrast to *cis*-PA, *trans*-PA is characterised by a steeper initial section of the  $N(T)$  curve at  $T < T_c$ . [The quantity  $n$  in Eqn (4) varies from 1 to 4 for the *trans*-PA specimens obtained] and reaches a plateau at  $T \leq 140$  K. The latter fact is analogous to the manifestation of the so called magnetic saturation. However, for the given temperature range, magnetic saturation may occur when the condition  $g\mu_B SB_0 > kT$  is fulfilled, i.e. for  $B_0 > 100$  T, which greatly exceeds the magnetic field strength  $B_0 \leq 5$  T used in our experiments. Most probably, this effect may be induced by the significant increase in the concentration of neutral solitons with an amplitude  $A$  and hence by the shortening of the inter-radical distance  $R$  and the intensification of the interaction between these charge carriers with the probability  $W_R \sim A \exp(-2AR)$ .<sup>58</sup> Furthermore, the ‘unfreezing’ of the 1D-diffusion of a proportion of solitons at a rate  $\nu_{1D}$  leads to an additional increase in the probability of the intersoliton interaction  $W_{SS} \sim \nu_{1D} \sim \nu_{1D}^0 T^{-2}$  (see below). As a consequence of the overlap of the wave functions of the unpaired electrons of neighbouring solitons, their discrete levels, located in the energy gap, are broadened and transformed into a soliton band of finite width. As in the case of *cis*-PA, the constants  $A$ ,  $B$ , and  $n$  are determined by the different properties of the *trans*-isomer.

The study of *trans*-PA specimens lightly doped with iodine vapour has shown<sup>54</sup> that the form of the spectra and the ratio of the concentrations of the mobile and localised paramagnetic centres do not vary. This finding agrees with the earlier hypothesis<sup>45</sup> of the existence in *trans*-PA of both mobile solitons and solitons trapped in short conjugated sections of the chain. Although the paramagnetic centres indicated do in fact have different mobilities, in the course of the doping process they acquire a charge with equal probabilities and become diamagnetic.

The magnetic properties of PA thus depend significantly both on the conformation of the polymer chains and on the concentration and mobility of the neutral solitons. In the *cis*–*trans* isomerisation of the initial PA specimen, the concentration of the trapped solitons increases appreciably and mobile charge carriers appear. The ‘unfreezing’ of the mobility of a small proportion of the solitons does in fact increase the conductivity of the film by several orders of magnitude. The transition to high fields for the recording of the EPR spectra increases significantly the resolution of the method and diminishes the probability of the

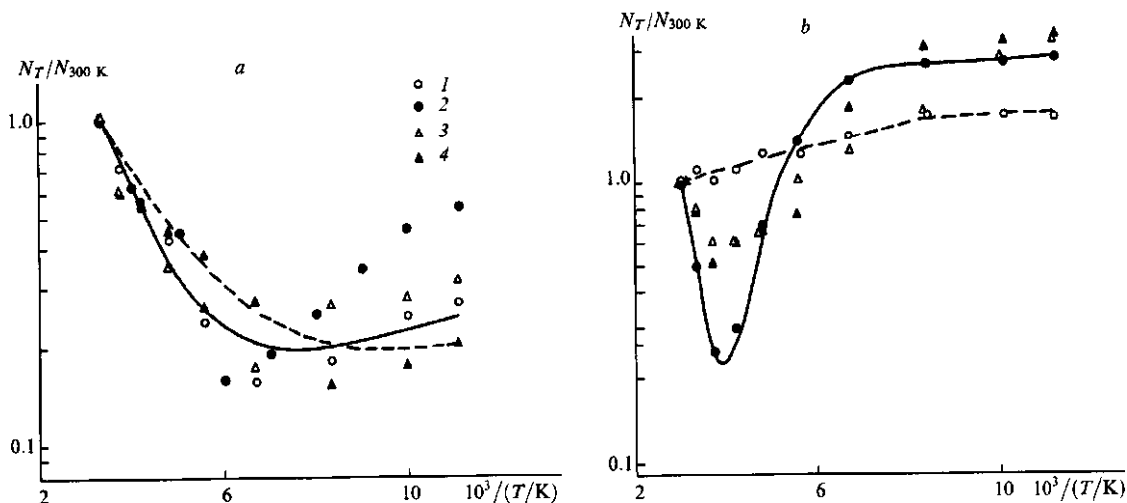


Figure 3. Temperature dependences of the concentrations of the paramagnetic centres in specimens 2 (1), 4 (2), 6 (3), and 5 (4) (Table 2) of (a) *cis*- and (b) *trans*-polyacetylenes relative to values measured at room temperature.

interaction between paramagnetic centres having different mobilities, which makes it possible to analyse more correctly and accurately the magnetic properties of the localised and delocalised solitons in PA.

### III. Passage effects and the electronic relaxation of the charge carriers in polyacetylene

With increase of the amplitude of the magnetic component of the UHF field  $B_1$ , dome-shaped components with a Gaussian distribution of the spin packets were recorded in the 2 mm EPR spectra of *cis*- and *trans*-PA (Fig. 4).<sup>54,59</sup> The intensity and form of these components depend on the amplitude  $B_m$  and the frequency  $\omega_m$  of the HF modulation, the quantity  $B_1$ , and the relaxation times of the paramagnetic centres. The appearance of these signals is associated with the manifestation of the effects of the rapid adiabatic passage of a nonuniformly ordered line.<sup>60</sup> Such passage effects had not been recorded previously in the study of PA in the frequency range  $\nu_e \leq 37$  GHz.<sup>16</sup> The following explanation of this finding can be put forward. The form of an individual spin packet in PA is determined by a set of time characteristics:  $\tau_1$ ,  $\tau_2$ ,  $(\gamma_e \Delta B_{PP})^{-1}$ ,  $\omega_m^{-1}$ ,  $(\gamma_e B_m)^{-1}$ ,  $(\gamma_e B_1)^{-1}$ , and  $B_1(dB_0/dt)^{-1}$ .

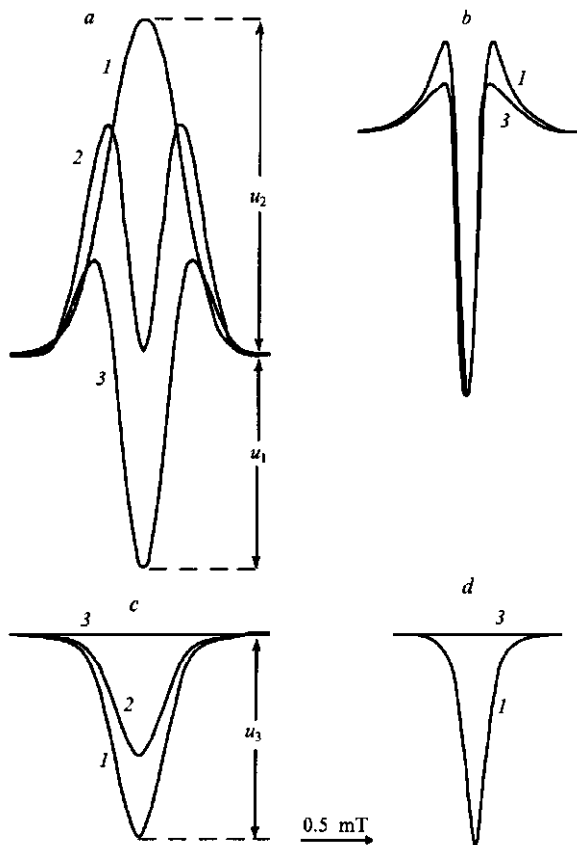


Figure 4. In-phase (a, b) and quadrature (c, d) components of the first derivatives of the dispersion signals of specimens of *cis*- (a, c) and *trans*-PA (b, d) recorded in the two-millimetre EPR range for different values of  $B_1$  (mT): (1) 0.2; (2) 0.2–20; (3) 20.

On transition to high magnetic fields, the probability of the cross-relaxation of the paramagnetic centres with  $s = \frac{1}{2}$  and  $g \approx 2$ , localised at a distance  $r_{1,2}$ , diminishes in accordance with the law<sup>61</sup>

$$W_{cr} \sim r_{1,2}^{-3} \exp(-0.25 B_0^2 r_{1,2}^6 \mu_B^{-2}),$$

as a consequence of which the interaction between the spin packets diminishes and they may be saturated under the usual experimental conditions. When the conditions for the saturation of the signal [ $s = \gamma_e B_1 (\tau_1 \tau_2)^{1/2} \geq 1$ ] and for the adiabatic nature of the passage of its envelope ( $\gamma_e \omega_m B_m \ll \gamma_e^2 B_1^2$ ) are fulfilled and also when the signal passage time exceeds the effective relaxation time  $\tau = (\tau_1 \tau_2)^{1/2}$ , i.e.  $B_1(dB_0/dt)^{-1} \gg \tau$ , there is insufficient time for the relaxation processes to influence significantly the nature of the motion of the magnetisation vector  $M$  of the paramagnetic centres during the period of its precession around the direction  $B_m$ . The repeated passage through resonance leads to the establishment of a stationary trajectory of the vector  $M$  and to the appearance of three components ( $u_1, u_2, u_3$ ) of the dispersion signal  $U$  with the shape function  $g(\nu_e)$ .<sup>62</sup>

$$U = u_1 g'(\nu_e) \sin(\omega_m t) + u_2 g(\nu_e) \sin(\omega_m t - \pi) + u_3 g(\nu_e) \sin(\omega_m t \pm \pi \frac{1}{2}), \quad (5)$$

along the  $z$ ,  $-z$ , and  $-x$  axes respectively. These components can be recorded separately with the appropriate tuning of the phase detector of the instrument. The contribution of each component  $u_i$  depends on the ratio of  $\tau$  to the rate of passage through resonance  $B_1(dB_0/dt)^{-1}$ . Evidently  $u_2 = u_3 = 0$  when  $s \ll 1$ . In this case, the classical  $u_1$  dispersion signal is recorded. When the inequality  $B_1(dB_0/dt)^{-1} \geq \tau$  holds, the vector  $M$  has sufficient time to relax to the equilibrium state during each modulation period and the  $U$  dispersion signal is determined mainly by the components  $u_1 g'(\omega_e)$  and  $u_3 g(\omega_e)$  with the intensities at the centre of the spectrum (for  $\nu = \nu_e$ )

$$u_1 = M_0 \pi \gamma_e^2 B_1 B_m \quad \text{and} \quad u_3 = \frac{1}{2} M_0 \pi \gamma_e^2 B_1 B_m \tau_1 \tau_2.$$

At a low rate of relaxation, the spin 'sees' only an average applied field and the signal is described by the integral terms of Eqn (5) with the central intensities

$$u_2 = \frac{1}{2} M_0 \pi \gamma_e^2 B_1 B_m \tau_2 \quad \text{and} \quad u_3 = M_0 \pi \gamma_e^2 B_1 B_m \tau_2 (4 \omega_m \tau_1)^{-1}.$$

The case  $\omega_m \tau_1 > 1$  occurs for *cis*-PA, so that the dispersion signal is determined mainly by the last two terms of Eqn (5). Calculations have shown<sup>54,59</sup> that in this case the relaxation times may be calculated from the ratio of the central amplitudes of these components by means of the following formulae:

$$\tau_1 = \frac{3 \omega_m (1 + 6 \Omega)}{\gamma_e^2 B_{10}^2 \Omega (1 + \Omega)}, \quad (6a)$$

$$\tau_2 = \frac{\Omega}{\omega_m}, \quad (6b)$$

where  $\Omega = u_3 u_2^{-1}$ , and  $B_{10}$  is the value of the component  $B_1$  for which the condition  $u_1 = -u_2$  holds.

In the EPR spectra of *trans*-PA, the passage effects are manifested to a much lesser extent (Fig. 4). The condition  $\omega_m \tau_1 < 1$  holds for this substance, so that the relaxation times can be calculated by the formulae<sup>54,59</sup>

$$\tau_1 = \frac{\pi u_3}{2 \omega_m u_1}, \quad (7a)$$

$$\tau_2 = \frac{\pi u_3}{2 \omega_m (u_1 + 11 u_2)}. \quad (7b)$$

The temperature dependences of the quantities  $\tau_1$  and  $\tau_2$ , determined from the 2 mm EPR spectra of the specimens of *cis*- and *trans*-PA of different thickness and obtained under different conditions of synthesis, are presented in Table 2 in the functional form  $\tau_{1,2} = AT^\alpha$ . Fig. 5 presents the functions  $\tau_1(T)$  and  $\tau_2(T)$  for

**Table 2.** Temperature dependences of the relaxation times [ $\tau_{1,2} = AT^\alpha$ (s)] for different *cis*- and *trans*-polyacetylene specimens.

Specimen	$\tau_1$		$\tau_2$			$\tau_1$		$\tau_2$	
	A	$\alpha$	A	$\alpha$		A	$\alpha$	A	$\alpha$
<i>cis</i> -PA					<i>trans</i> -PA				
1	0.04	-1.6	$1.8 \times 10^{-9}$	1.2	2.7	-2.6	$1.0 \times 10^{-7}$	0.5	
1 <sup>a</sup>	0.37	-2.0	$7.7 \times 10^{-9}$	1.0	—	—	—	—	
2	0.006	-1.4	$1.5 \times 10^{-7}$	0.5	0.1	-2.2	$7.2 \times 10^{-8}$	0.3	
2 <sup>a</sup>	0.77	-2.3	$1.0 \times 10^{-7}$	0.5	—	—	—	—	
3	1.4	-2.3	$9.5 \times 10^{-8}$	0.5	$2.0 \times 10^{-3}$	-1.7	$1.3 \times 10^{-5}$	-0.9	
3 <sup>a</sup>	290	-3.3	$1.7 \times 10^{-8}$	0.8	—	—	—	—	
3 <sup>b</sup>	52	-2.7	$1.2 \times 10^{-8}$	0.8	—	—	—	—	
3 <sup>ab</sup>	6.5	-3.6	$4.2 \times 10^{-9}$	1.0	—	—	—	—	
3 <sup>c</sup>	—	—	—	—	62	-3.5	2.1	-3.0	
4	0.65	-2.1	$9.6 \times 10^{-9}$	0.9	$4.0 \times 10^{-3}$	-1.5	$2.9 \times 10^{-6}$	-1.0	
4 <sup>a</sup>	10	-2.6	$2.8 \times 10^{-9}$	1.1	—	—	—	—	
5	27	-2.5	$2.4 \times 10^{-7}$	0.3	$4.0 \times 10^{-4}$	-1.2	$9.1 \times 10^{-6}$	-0.7	
5 <sup>d</sup>	—	—	—	—	$8.3 \times 10^{-4}$	-1.3	$5.0 \times 10^{-6}$	-0.6	
6	3125	-3.5	$3.4 \times 10^{-8}$	0.7	$1.7 \times 10^{-4}$	-1.1	$1.0 \times 10^{-6}$	-0.8	
7	1587	-2.7	$4.2 \times 10^{-9}$	1.0	$1.1 \times 10^{-2}$	-1.9	$9.1 \times 10^{-5}$	-1.2	
8	833	-2.6	$9.1 \times 10^{-9}$	0.9	$2.8 \times 10^{-4}$	-1.0	$2.2 \times 10^{-5}$	-0.7	
8 <sup>c</sup>	83	-2.7	$3.6 \times 10^{-9}$	1.1	—	—	—	—	

Remarks. The measurements were performed

<sup>a</sup> in the presence of atmospheric oxygen,

<sup>b</sup> after storage for 6 months under an inert atmosphere,

<sup>c</sup> after doping with iodine vapour up to  $\sigma_{dc} \approx 10 \text{ S m}^{-1}$ ,

<sup>d</sup> after annealing under an inert atmosphere. Specimens 1–8 investigated were obtained under different conditions and had different thicknesses.

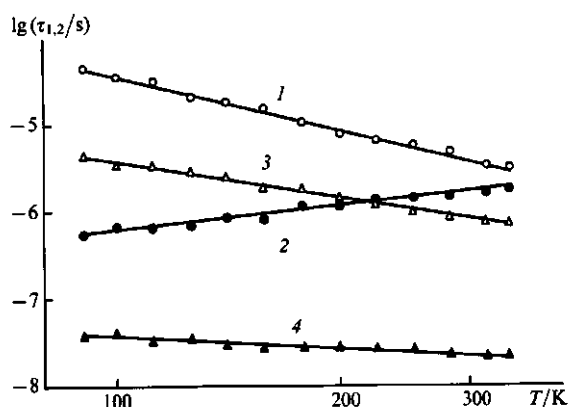


**Figure 5.** Temperature dependences of the spin-lattice ( $\tau_1$ ) (lines 1 and 3) and spin-spin ( $\tau_2$ ) (lines 2 and 4) relaxation times of *cis*- (lines 1 and 2) and *trans*-polyacetylenes (lines 3 and 4).

the *cis*- and *trans*-isomers of PA (No. 4 in Table 2). It is seen from the data presented that the spin-lattice relaxation times of the paramagnetic centres in both isomers diminish monotonically with increase in temperature, whereas the spin-spin relaxation times exhibit different temperature dependences in the case of *cis*- and *trans*-PA.

It is necessary to note that the PA relaxation times are effective relaxation times of the localised and mobile paramagnetic centres. Therefore, under the conditions where the dipole-dipole interactions of the paramagnetic centres in PA predominate, one can write

$$\left(\frac{1}{\tau_{1,2}}\right)_{cis} \approx \left(\frac{1}{\tau_{1,2}}\right)_{loc}, \quad (8a)$$

$$\left(\frac{n}{\tau_{1,2}}\right)_{trans} \approx \left(\frac{n_1}{\tau_{1,2}}\right)_{loc} + \left(\frac{n_2}{\tau_{1,2}}\right)_{mob}, \quad (8b)$$

where  $n = n_1 + n_2$ . This makes it possible to determine separately the relaxation times of paramagnetic centres with different mobilities in *trans*-PA, using the experimental quantities  $\tau_1$ ,  $\tau_2$ ,  $n$ , and  $n_1/n_2$ .

If the spin-lattice relaxation time is formulated as  $\tau_1 = An^{-\alpha}v_c^\beta T^{-\gamma}$  ( $A$  is a constant), then  $\alpha$  varies from 0.7 to 1.0 in the temperature range from 330 to 90 K,  $\beta$  is 3 for *cis*-PA and -0.5 for *trans*-PA, and  $\gamma$  varies from 1.4 to 3.5 for *cis*-PA and from 1.0 to 2.6 for *trans*-PA depending on the thickness of the specimen (Table 2). This shows that mainly Raman two-phonon relaxation processes occur in *cis*-PA,<sup>61</sup> whereas more complex spin-lattice interactions take place in *trans*-PA. The latter factor may be accounted for by the fact that a joint Raman spin-lattice 1D- and 3D-interaction of the immobilised spins with an overall probability<sup>63</sup>

$$W_R \sim k_1 n_1 v_c^{-1} T^2 + k_2 n_1 v_c^{-1} T,$$

( $k_1$  and  $k_2$  are constants) and diffusional modulation of the spin-lattice interaction by the 1D-motion of some of the neutral solitons with a probability  $W_D \sim v_c^{1/2}$  take place in *trans*-PA.<sup>64</sup>

Table 3 presents the temperature dependences of the relaxation times of *cis*- and *trans*-PA specimens (No. 8, Table 2) partly oriented by stretching. The data presented demonstrate convincingly that the relaxation times  $\tau_1(T)$  and  $\tau_2(T)$  of the oriented *cis*-PA vary only slightly with the angle  $\psi$  between the direction of the external magnetic field and the direction of stretching of the specimen, whereas for the oriented *trans*-PA film the relaxation times are functions of the angle  $\psi$  as a result of the 1D-diffusion of a paramagnetic centre of finite extent within the film.

It is essential to note that the relaxation times are important parameters of PA, characterising its structural and conducting properties. Thus it has been shown<sup>65</sup> that an increase in molecular mass diminishes the electronic spin-lattice relaxation time of the paramagnetic centres in PA. This parameter should therefore be sensitive to the degradation of the polymer. Indeed, the storage of the initial *cis*-PA specimen for six months under an inert atmosphere leads to a significant increase in  $\tau_1$  owing to its partial degradation (Fig. 6).<sup>54,59</sup>

A similar change in  $\tau_1$  is observed on irradiation of this specimen with a beam of fast electrons at a dose of 1 MGy.

**Table 3.** Temperature dependences of the relaxation times [ $\tau_{1,2} = AT^{\alpha}(s)$ ] of specimens 8 (Table 2) of *cis*- and *trans*-PA, partly oriented by stretching, as a function of the direction of stretching in the external magnetic field.

$\psi/\text{deg}$	$\tau_1$		$\tau_2$		$\tau_1$		$\tau_2$	
	$A$	$\alpha$	$A$	$\alpha$	$A$	$\alpha$	$A$	$\alpha$
	<i>cis</i> -PA				<i>trans</i> -PA			
0	0.04	-1.2	$4.0 \times 10^{-8}$	0.6	$2.1 \times 10^{-2}$	-2.0	$2.4 \times 10^{-3}$	-1.7
30	—	—	—	—	$5.0 \times 10^{-4}$	-1.2	$1.0 \times 10^{-5}$	-0.5
60	—	—	—	—	$2.8 \times 10^{-3}$	-1.4	$1.5 \times 10^{-5}$	-0.5
90	0.16	-1.5	$2.7 \times 10^{-8}$	0.7	$3.5 \times 10^{-5}$	-0.5	$5.2 \times 10^{-5}$	-0.8

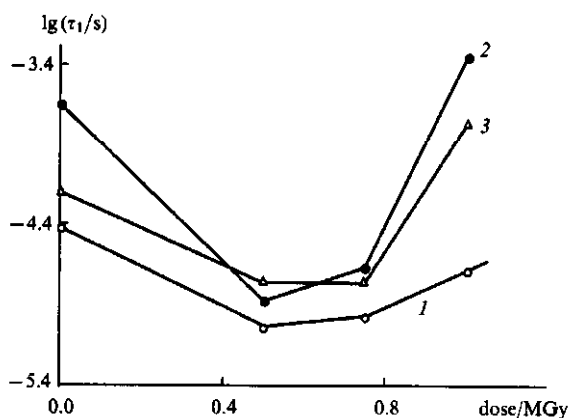


**Figure 6.** Dependence of the spin-lattice relaxation time  $\tau_1$  ( $T = 120$  K) for the initial *cis*-PA specimen (specimen 3 in Table 2, curve 1) and after its storage under an inert atmosphere for 6 months (line 2) and 12 months (line 3) as a function of the dose of irradiation by a beam of fast electrons.

However, on irradiation of the specimen with an electron beam at a dose of 0.50–0.75 MGy, the time  $\tau_1$  remains virtually constant during the above period of storage (Fig. 6). After more prolonged storage of the initial specimen and the specimen irradiated with a dose of 1 MGy,  $\tau_1$  diminishes somewhat, which may be attributed to some increase in the length of the chains and to the *cis*–*trans* isomerisation of PA. This phenomenon demonstrates the possibility of the effective stabilisation and even an improvement of the electrodynamic characteristics of *cis*-PA when the latter is irradiated with the optimum dose.

The increase in the concentration of paramagnetic centres on *cis*–*trans* isomerisation of PA accelerates the spin-lattice relaxation. Since in massive PA films with a low-density of the polymer chains such isomerisation proceeds most readily, longer *trans*-sections with an increased rigidity are formed in them, and is accompanied by an increase in the activation energy for the libration of the chains ( $E_a$ ). The latter quantity may be determined by analysing the temperature dependence of the width of the spectral line of a trapped soliton.<sup>54</sup> Since the unpaired electron, delocalised within the limits of a neutral mobile soliton, has a finite density  $\rho(n)$  on  $N$  hydrogen nuclei, there is a possibility of their hyperfine interaction. In this case the effective width of the delocalisation of the unpaired electron  $N = \rho(n)^{-1}$  in *trans*-PA can be found from the equation for the Gaussian component of the line width<sup>66</sup>  $\Delta B_{pp}^G \approx N^{1/2} \rho(n)$  subject to the condition  $\sum \rho(n) = 1$ .

Figure 7 presents the  $\tau_1 - N - E_a$  correlations for *trans*-PA specimens of different thicknesses. It is seen from the figure that, as the specimen becomes more massive, a tendency is observed towards the acceleration of the spin-lattice relaxation processes and towards an increase in the activation energy for the libration of the polymer chains. This constitutes additional evidence for the increase in rigidity, packing density, and length of the *trans* chains with increase in the thickness of the *trans*-PA specimen.

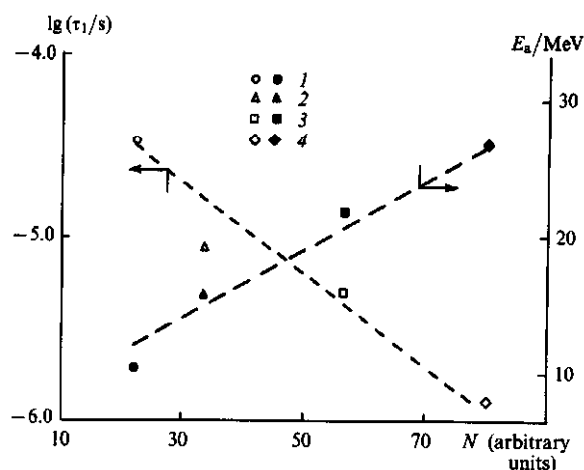


**Figure 7.** Dependence of the spin-lattice relaxation time  $\tau_1$  ( $T = 80$  K) and the activation energy for the librations of the chains  $E_a$  on the effective spin delocalisation length  $N$  in *trans*-PA specimens with different thicknesses ( $\mu\text{m}$ ): (1) 90; (2) 110; (3) 350; (4) 180.

The correlations presented are useful for the standardisation of *trans*-PA films.

It is essential to note that a light doping of *trans*-PA with iodine vapour (up to  $\sigma_{ac} \approx 10 \text{ S m}^{-1}$ ) leads to a fourfold decrease in the overall spin concentration and to a decrease in  $\tau_2$  approximately by an order of magnitude (Table 2). Some change in  $\tau_1$  occurs on diffusion of atmospheric oxygen into the *trans*-PA matrix. Taking into account the concentration dependence of this quantity, one may conclude that the introduction of  $\text{I}_2$  and  $\text{O}_2$  molecules reduces the packing density of the PA chains and increases the number of traps for mobile solitons.

#### IV. Dynamics of the soliton and the mechanism of charge transfer in *trans*-polyacetylene

The diffusion of the soliton along the polymer chain is characterised by the translational propagator of motion  $P_{tr}(r, r_0, \tau)$ . If in the initial instant the  $j$ th particle is located at a point  $r_0$  relative to the  $i$ th particle, then the propagator defines the probability that at the instant  $t = \tau$  the  $i$ th particle is located in the region  $r + dr$  relative to the new position of the  $j$ th particle.

For the Brownian model of diffusional motion, the propagator  $P_{tr}(r, r_0, \tau)$  constitutes the solution of the familiar equation

$$\frac{\partial P_{tr}(r, r_0, t)}{\partial t} = D_{tr} \Delta P(r, r_0, t), \quad (9)$$

subject to the initial condition  $P_{tr}(r, r_0, t) = \delta(r - r_0)$ , where  $D_{tr} = [D_i]$ ,  $D_i = v_i c_i$  is the diffusion coefficient,  $v_i$  is the rate of diffusion,  $c_i$  is a constant introduced owing to the discrete nature of the system, and  $\hat{i}$  is a unit vector of the molecular coordinate system. In an explicit form, the above propagator for a 1D-system is given by the following relation:<sup>67</sup>



$$P(r, r_0, \tau)_{1D} = (4\pi v_{\parallel} \tau)^{-1/2} \exp\left[-\frac{(r-r_0)^2}{4v_{\parallel} c_{\parallel}^2 \tau}\right] \exp(-v_{\perp} \tau), \quad (10)$$

where  $v_{\parallel}$  and  $v_{\perp}$  are the rates of spin diffusion along the polymer chain and between the chains respectively.

The diffusing soliton induces a local magnetic field  $B_{loc}(t)$  at the sites of other electron or nuclear spins, thereby influencing the electronic relaxation times of neighbouring spins. The following general expression may be written for the relaxation time:

$$\tau_{1,2} = f[J(\omega)],$$

where  $J(\omega)$  is a function of the spectral density given by

$$J(\omega) = \int_{-\infty}^{+\infty} G(\tau) \exp(-i\omega\tau) d\tau. \quad (11)$$

The autocorrelation function of the oscillating local field  $B_{loc}(t)$  for a discrete system is

$$G(\tau) = c_i \sum \sum A(r_0, t) P(r, r_0, \tau) F(r_0) F^*(r) dr_0 dr, \quad (12)$$

where  $c_i$  is the lattice constant for the discrete system,  $A(r, t)$  the probability of finding the spin at a distance  $r$  at time  $t$ , equal to the spin concentration per monomer unit  $n$ , and  $F(r)$  is the probability of finding two spins at a distance  $r$  at time  $t$ .

For frequencies  $\omega \ll v_{\parallel} c_{\parallel}^2 (r-r_0)^{-2}$ , the spectral density function can assume the following form:

$$J(\omega) = n J_{1D}(\omega) \sum \sum F(r_0) F^*(r) f_{1D}(|r-r_0|), \quad (13)$$

where  $n = n_1 + \sqrt{2n_2}$  is the probability of finding the spin in the initial instant in the position  $r_1$ ,  $J_{1D}(\omega) = (2\pi v_{\parallel} v_e)^{-1/2}$  for  $v_{\perp} \ll v_e \ll v_{\parallel}$ , and  $J_{1D}(\omega) = (2\pi v_{\parallel} v_{\perp})^{-1/2}$  for  $v_{\perp} \gg v_e$ . The expression under the summation sign $\ddagger$  can be written in the form

$$F(r_0) F^*(r) f_{1D}(|r-r_0|) = \frac{(3 \cos^2 \vartheta - 1)^2}{r_1^2 r_2^2},$$

where  $\vartheta$  is the angle between the vectors  $r_1$  and  $r_2$ .

Since PA is characterised mainly by an anisotropic dipolar (and to a lesser extent by an isotropic scalar) hyperfine interaction of the electron ( $S$ ) and nuclear ( $I$ ) spins, in the case of the dipolar interaction between equivalent spins ( $S = I$ ), the equations for the rates of electronic relaxation in a polycrystalline specimen can be written in the form<sup>67</sup>

$$\tau_1^{-1} = \langle \Delta\omega^2 \rangle [J(\omega_e) + 4J(2\omega_e)], \quad (14a)$$

$$\tau_2^{-1} = \frac{1}{2} \langle \Delta\omega^2 \rangle [3J(0) + 5J(\omega_e) + 2J(2\omega_e)], \quad (14b)$$

where

$$\langle \Delta\omega^2 \rangle = \frac{1}{5} \left( \frac{\mu_0}{4\pi} \right)^2 \gamma_e^4 \hbar^2 S(S+1) n \sum \sum$$

(here  $\omega_e$  is the frequency of the precession of the electron spin and  $m_0$  is the magnetic permeability *in vacuo*).

The anisotropic hyperfine interaction accelerates the electronic relaxation by the amounts

$$\begin{aligned} \tau_1^{-1} = & \frac{1}{15} a^2 I(I+1) n \sum \sum [J(\omega_e - \omega_I) + 3J(\omega_e) \\ & + 6J(\omega_e + \omega_I)] + \frac{1}{15} a^2 S(S+1) n \sum \sum [-J(\omega_e - \omega_I) \\ & + 6J(\omega_e + \omega_I)] \frac{\langle I_z \rangle - I_0}{\langle S_z \rangle - S_0}, \end{aligned} \quad (15a)$$

$\ddagger$  Henceforth double summation will be designated for simplicity by  $\sum \sum$ .

$$\begin{aligned} \tau_2^{-1} = & \frac{1}{30} a^2 I(I+1) n \sum \sum [4J(0) + J(\omega_e - \omega_I) \\ & + 3J(\omega_e) + 6J(\omega_I) + 6J(\omega_e + \omega_I)], \end{aligned} \quad (15b)$$

( $\omega_I$  is the frequency of the precession of the nuclear spin and  $a = \mu_0 \gamma_e \gamma_I \hbar / 8\pi$  is the hyperfine interaction constant), whereas the isotropic interactions of the electron and nuclear spins make an additional contribution to the rate of electronic relaxation:

$$\tau_1^{-1} = \frac{1}{3} n_p a^2 I(I+1) J(\omega_e - \omega_I) \left[ 1 - \frac{S(S+1)(\langle I_z \rangle - I_0)}{I(I+1)(\langle S_z \rangle - S_0)} \right] \quad (16a)$$

$$\tau_2^{-1} = \frac{1}{6} n_p a^2 I(I+1) [J(0) + J(\omega_e - \omega_I)]. \quad (16b)$$

By setting the expression under the summation sum in Eqn (14) equal to  $2 \times 10^{58} \text{ m}^{-6}$  and that in Eqn (15) to  $2.8 \times 10^{59} \text{ m}^{-6}$  and also assuming that  $(\langle I_z \rangle - I_0)(\langle S_z \rangle - S_0)^{-1} = 0.078$ ,<sup>35</sup> one can formulate simpler expressions for the rate of relaxation of *trans*-PA with randomly oriented polymer chains:<sup>56</sup>

$$\tau_1^{-1} = 1.3 \times 10^{16} (v_e v'_{1D})^{-1/2} (2.7 \times 10^4 n + 1), \quad (17a)$$

$$\begin{aligned} \tau_2^{-1} = & 6.3 \times 10^{15} v_{1D}^{-1/2} [(7.6 \times 10^9 n + 3.4 \times 10^5) v_{3D}^{-1/2} \\ & + (4.3 \times 10^4 n + 1) v_e^{-1/2}]. \end{aligned} \quad (17b)$$

In the case of the predominantly dipole-dipole interaction of the paramagnetic centres, the equations for the rates of relaxation of the partly oriented *trans*-PA with a degree of orientation of the polymer chains  $A$  consist of two components:

$$\begin{aligned} \tau_1^{-1} = & A \langle \Delta\omega^2 \rangle [J(\omega_e) P_1 + 4J(2\omega_e) P_2] \\ & + (1-A) \langle \Delta\omega^2 \rangle [J(\omega_e) P'_1 + 4J(2\omega_e) P'_2], \end{aligned} \quad (18a)$$

$$\begin{aligned} \tau_2^{-1} = & \frac{A}{2} \langle \Delta\omega^2 \rangle [3J(0) P_0 + 5J(\omega_e) P_1 + 2J(2\omega_e) P_2] \\ & + \frac{(1-A)}{2} \langle \Delta\omega^2 \rangle [3J(0) P'_0 \\ & + 5J(\omega_e) P'_1 + 2J(2\omega_e) P'_2], \end{aligned} \quad (18b)$$

where the constants  $P_i$  and  $P'_i$  correspond to the oriented and randomly disposed polymer chains respectively.

If we put  $P_0 = 4.3 \times 10^{58} \sin^4 \psi$ ,  $P_1 = 4.8 \times 10^{57} (1 - \cos^4 \psi)$ ,  $P_2 = 4.8 \times 10^{57} (1 + 6 \cos^2 \psi + \cos^4 \psi)$ ,  $P'_0 = 1.6 \times 10^{58}$ ,  $P'_1 = 2.7 \times 10^{57}$ , and  $P'_2 = 1.1 \times 10^{58} \text{ m}^{-6}$ ,<sup>27</sup> Eqns (18) can be written in a simpler form:

$$\begin{aligned} \tau_1^{-1} = & 5.0 \times 10^{19} n (v_e v'_{1D})^{-1/2} \\ & \times [6.8 - A(1.1 - 14.0 \cos^2 \psi + \cos^4 \psi)], \end{aligned} \quad (19a)$$

$$\begin{aligned} \tau_2^{-1} = & 2.8 \times 10^{20} n v_{1D}^{-1/2} \{ (1-A + A \sin \psi) v_{3D}^{-1/2} \\ & + [2.1 + A(1.1 + 1.3 \cos^2 \psi - 2.9 \cos^4 \psi)] v_e^{-1/2} \}. \end{aligned} \quad (19b)$$

Figure 8 presents the temperature variations of the rates of diffusion  $v_{1D}$  and  $v_{3D}$  calculated for the initial *trans*-PA specimen ( $A = 0$ ) (specimen 8 in Table 2) and for the same specimen with polymer chains partly oriented by stretching ( $A = 0.07$ ).

When the unpaired electron is delocalised over 15 carbon nuclei, the rate of 1D-diffusion of the soliton in the initial *trans*-PA specimen is  $v_{1D} = 0.25 v_{1D} N^2 \leq 5.6 \times 10^{11} \text{ Hz}$  at room temperature. The latter quantity is approximately two orders of magnitude smaller than that obtained earlier by magnetic resonance methods.<sup>22,35</sup> Furthermore, the relation  $v'_{1D}(T) \sim T^{-2}$  does not agree with the existing theoretical ideas.<sup>13,14</sup> The anisotropy of the spin dynamics depends only slightly on

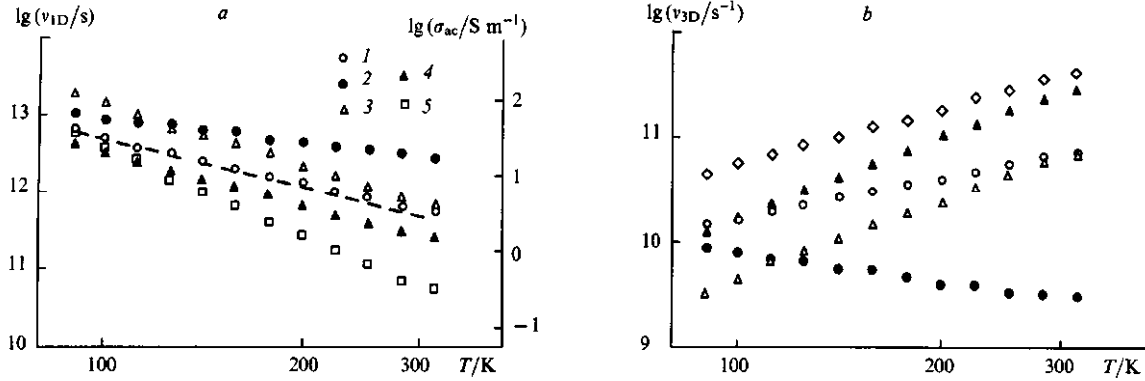


Figure 8. Logarithmic temperature dependences of the quantities  $v_{1D}$  (a) and  $v_{3D}$  (b) for a neutral soliton in the initial (line 1) and partly oriented ( $A = 0.07$ ) *trans*-PA with the crystallographic  $c$  axes oriented at the angles

$\psi = 90^\circ$  (line 2),  $60^\circ$  (line 3),  $30^\circ$  (line 4), and  $0^\circ$  (line 5) relative to the external magnetic field. The temperature dependence of the quantity  $\sigma_{ac}$ , calculated by Eqn (20b) for  $v_e = 1.4 \times 10^{11}$  Hz, is shown by a dashed line.

temperature and amounts to  $v'_{1D}v_{3D}^{-1} \geq 30$  in this specimen and to  $10-10^4$  in other *trans*-PA specimens,<sup>56</sup> which is significantly less than the values obtained previously.<sup>22,35</sup>

If the rates of spin diffusion are expressed in the form  $v_{1D} = AT^{-\alpha}$  and  $v_{3D} = BT^\beta$ , then the increase in the anisotropy of the spin diffusion by three orders of magnitude in different specimens is accompanied by the simultaneous increase in the quantities  $\alpha$  (from 2 to 5) and  $\beta$  (from 0.4 to 7) at room temperature. When *trans*-PA is doped, it becomes disordered and the Coulombic and confinement trapping of the charge carriers increase.<sup>19</sup> However, if these factors are neglected and it is supposed that all the mobile carriers with the mobility  $\mu$  participate in the charge transfer process, then the conductivity of *trans*-PA, calculated from the equation  $\sigma = Ne\mu = Ne^2v_{1D}c_{\parallel}^2k^{-1}T^{-1}$  ( $e$  is the electronic charge), does not exceed  $0.02 \text{ S m}^{-1}$  at room temperature, which is several orders of magnitude less than the value usually attainable for heavily doped *trans*-PA.<sup>1-3</sup> Furthermore, even light doping leads to a significant alteration of the frequencies of spin diffusion in *trans*-PA (Fig. 9). Hence it follows that, in order to attain a high conductivity of the polymer, the condition of the multiple charge transfer by each soliton within a limited section of the polymer chain must be fulfilled.

The dynamic properties of solitons can be described more correctly within the framework of the formal treatment involving the isoenergetic intersoliton charge transfer proposed by Kivelson.<sup>11</sup> The essential feature of the method consists of the phonon-assisted interchain tunnelling of the charge between the energy levels of the solitons, based on the Coulombic interaction

of the solitons having a charge  $q_1$  with ions having the opposite charge  $q_2$  present in the undoped and lightly doped *trans*-PA. The excess charge  $\Delta q = q_1 - q_2$  may undergo a phonon-assisted transfer, with a finite probability, to a neutral soliton moving along a neighbouring polymer chain. If at the instant of such transfer the neutral soliton is also located close to a charged ion, the energy of the charge carrier before and after charge transfer remains unaltered. In this case, the conductivity of the polymer (the d.c. conductivity  $\sigma_{dc}$  and the a.c. conductivity  $\sigma_{ac}$ ) is determined by the probability that the neutral soliton is located near an ion and also by the probability of finding its initial and final energies within the limits of  $kT$ .<sup>11</sup>

$$\sigma_{dc} = k_1 e^2 \frac{\gamma(T) \xi n_n n_{ch}}{k T N R_0^2 (n_n + n_{ch})^2} \exp\left(-\frac{2k_2 R_0}{\xi}\right) = \sigma_0 T^n, \quad (20a)$$

$$\begin{aligned} \sigma_{ac} &= \frac{e^2 n_i^2 n_0 (1 - n_0) \xi_{\parallel}^3 \xi_{\perp}^2 v_e}{384 k T} \left[ \ln \frac{4\pi v_e L_c}{n_0 (1 - n_0) \gamma(T)} \right]^4 \\ &= \frac{\sigma_0 v_e}{T} \left[ \ln \frac{k_3 v_e}{T^{n+1}} \right]^4. \end{aligned} \quad (20b)$$

Here  $\gamma(T)$  is the hopping frequency of the charge carriers,  $k_1$ ,  $k_2$ , and  $k_3$  are constants ( $k_1 = 0.45$ ,  $k_2 = 1.39$ ),  $\xi = (\xi_{\parallel} \xi_{\perp}^2)^{1/3}$ ,  $\xi_{\parallel}$  and  $\xi_{\perp}$  are the average parallel and perpendicular lengths of the soliton respectively,  $n_n$  and  $n_{ch}$  are the numbers of neutral and charged solitons per monomer unit,  $n_0$  is the relative content of the charged solitons,  $R_0 = (\frac{4}{3}\pi n_i)^{-1/3}$  is the average distance between inhomogeneities with a concentration  $n_i$ , and  $L_c$  is the degree of polymerisation or the number of monomer units in the polymer chain. A weak bond between the charge carriers and the polymer lattice is characteristic of the case under consideration, which results in the occurrence of hopping charge transfer between relatively remote states of the soliton. The temperature dependences presented above were obtained experimentally in a study of lightly doped *trans*-PA<sup>10,69</sup> and other conducting polymers.<sup>70,71</sup> Fig. 8 presents the temperature dependence of  $\sigma_{ac}$  calculated by Eqn (20b) with  $v_e = 1.4 \times 10^{11}$  Hz,  $n = 8.0$ ,  $k_3 = 2.9 \times 10^{23} \text{ sK}^9$ , and  $\sigma_0 = 9.3 \times 10^{-15} \text{ S s K m}^{-1}$  ( $\xi_{\parallel} = 1.0$ ,  $\xi_{\perp} = 0.25 \text{ nm}$ ,  $n_i = 1.3 \times 10^{25} \text{ m}^{-3}$ , and  $L_c = 2000$ )<sup>10,11,72,73</sup> for the initial *trans*-PA specimen. As can be seen from the figure, the  $v'_{1D}(T)$  and  $\sigma_{ac}(T)$  relations are quite satisfactorily correlated. Adopting  $\sigma_{dc} \sim 10^{-3} \text{ S m}^{-1}$  (see, for example, Epstein<sup>10</sup>) and  $\sigma_{ac} \sim 3 \text{ S m}^{-1}$  at  $T = 300 \text{ K}$  (Fig. 8), we obtain  $\sigma_{dc}/\sigma_{ac} \approx 3 \times 10^3$ , which agrees well with the value calculated<sup>10</sup> within the framework of Kivelson's theory<sup>11</sup>

$$\frac{\sigma_{ac}(v_e \rightarrow \infty)}{\sigma_{ac}(v_e \rightarrow 0)} \approx 10^4.$$

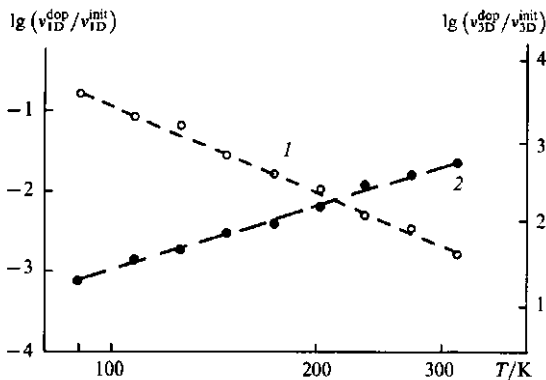


Figure 9. Temperature dependences of the ratios of the quantities  $v_{1D}$  (line 1) and  $v_{3D}$  (line 2) for a neutral soliton in the initial *trans*-PA to the corresponding values for a soliton in *trans*-PA doped with iodine up to  $\sigma_{dc} \approx 10 \text{ S m}^{-1}$ .

This confirms the applicability of the approach used to the interpretation of the transport properties of the soliton in *trans*-PA.

In the initial *trans*-PA specimen, the crystallographic  $c$  axes of the polymer chains are randomly oriented in space. It follows from Fig. 8 that, under the conditions of the orientational ordering of some of the polymer chains, the rates of the spin 1D- and 3D-diffusion are sensitive to the rotation of the specimen by an angle  $\psi$  in the external magnetic field, apparently owing to the finite length of the quasi-particles. The function  $v'_{1D}(\psi)$ , i.e.

$$\langle v'_{1D}(\psi) \rangle = v_{1D}^{\parallel}(\psi) \sin^2 \psi + v_{1D}^{\perp}(\psi) \cos^2 \psi, \quad (21)$$

where  $v_{1D}^{\parallel}(\psi)$  and  $v_{1D}^{\perp}(\psi)$  are extrema in the function  $v'_{1D}(\psi)$ , is in the antiphase relative to  $v_{3D}(\psi)$ . We may note that the effective spin diffusion can be described with the aid of a similar relation also in other low-dimensional systems.<sup>74, 75</sup> Thus the inequality  $v_{1D}^{\parallel}(\psi) \ll v_{1D}^{\perp}(\psi)$  is evidence for the delocalisation of the unpaired electron along the  $c$  axis within the limits of the soliton. Bearing in mind the fact that the soliton hops are limited by the interchain lattice constant and that the square of the length of the average diffusional hop along the  $c$  axis is  $0.25 \langle N^2 c^2 \rangle$ , the width of the soliton  $N$  can be calculated with the aid of the following simple equation:<sup>46</sup>

$$N^2 = \frac{4v_{1D}^{\perp}(\psi)}{v_{1D}^{\parallel}(\psi)}. \quad (22)$$

Figure 10 presents the temperature dependence of the width of the soliton calculated by Eqn (22) using the quantities  $v_{1D}^{\parallel}$  and  $v_{1D}^{\perp}$ , found graphically with the aid of Fig. 8. The value  $N = 14.8$  found for room temperature agrees well with the theoretical<sup>6</sup> and the earlier experimental<sup>45</sup> values of  $N$ . Extrapolation of the  $N(T)$  relation to lower temperatures makes it possible to determine the temperature ( $T_0 \approx 60$  K) at which the width of the soliton begins to increase. It is important to note that an anomaly in the function  $v'_{1D}(T)$  for *trans*-PA,<sup>37</sup> accounted for by a change in the mechanism of the electronic relaxation, has been recorded in precisely this temperature range.

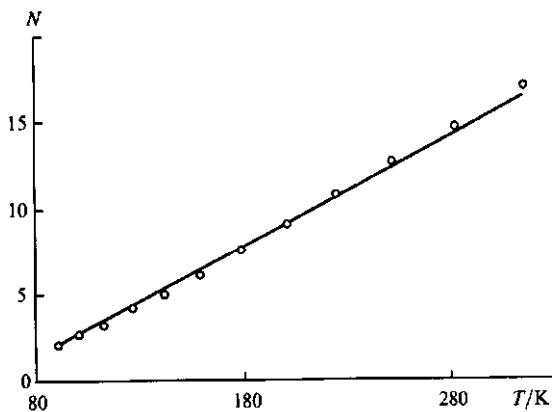


Figure 10. Temperature variation of the effective width  $N$  of the soliton in *trans*-PA.

Thus the experimental data indicate the 1D-diffusion of solitons into *trans*-PA at a rate appreciably exceeding the minimum rate  $v_{1D}^0$  calculated above by Eqn (1). This conclusion is confirmed also by the averaging of the components of the  $g$ -tensor of the mobile paramagnetic centres when condition (1) is fulfilled and by the narrowing of the line in the EPR spectrum of *trans*-PA over a wide frequency range in conformity with Eqn (3).

However, the most obvious evidence in support of the 1D-diffusion of the soliton is the sensitivity of the quantities  $v_{1D}$  and  $v_{3D}$  to the orientation of the polymer in the magnetic field.

The familiar Burgers–Korteweg–de Vries equation, describing the 1D-motion of unified waves in a nonlinear medium, assumes the form<sup>76</sup>

$$\frac{\partial u}{\partial t} + (v_{1D}^0 + \varepsilon u) \frac{\partial u}{\partial x} - \kappa \frac{\partial^2 u}{\partial x^2} + \beta \frac{\partial^3 u}{\partial x^3} = 0, \quad (23)$$

where  $\varepsilon$ ,  $\kappa$ , and  $\beta$  are the parameters of the nonlinearity, dissipation, and ‘reactive’ dispersion of the medium respectively. In a dissipative system with a low nonlinearity ( $\beta \approx 0$ ), there is a possibility of the formation of a mobile front (kink) with the difference  $u_2 - u_1$ . For such a quasi-particle, the stationary solution of Eqn (23) assumes the following form:

$$u(x, t) = 0.5(u_1 + u_2) - A \tanh\left(\frac{x - v_{1D}t}{2N}\right), \quad (24)$$

where

$$A = \frac{1}{2}(u_2 - u_1), \quad v_{1D} = v_{1D}^0 + \frac{1}{2}\varepsilon(u_1 + u_2), \quad \text{and} \quad N = \frac{\kappa}{2A\varepsilon},$$

are the amplitude, velocity, and width of the kink respectively. If the dissipation of the system is neglected ( $\kappa \approx 0$ ), then other quasi-particles—solitons—are stabilised in the system. For a family of such solitons, Eqn (23) has another integrable solution:

$$u(x, t) = A \operatorname{sech}^2\left(\frac{x - v_{1D}t}{N}\right), \quad (25)$$

where

$$v_{1D} = v_{1D}^0 + \frac{1}{3}A\varepsilon, \quad \text{and} \quad N^2 = \frac{3\beta}{A\varepsilon} = \frac{\beta}{v_{1D} - v_{1D}^0}.$$

It is essential to note that relations similar to Eqns (24) and (25) have been used<sup>6</sup> to describe nonlinear deformations of the lattice and electronic states of *trans*-PA.

The experimental<sup>46</sup> functional relations  $v_{1D}(T) \sim T^{-n}$  and  $N(T) \sim T^{n/2}$  ( $n \approx 2$ ) yield for *trans*-PA a relation of the type  $N^2 \sim v_{1D}^{-1}$ . This means that the motion of solitons in the given specimen, subject to the condition  $v_{1D} \ll v_{1D}^0 = 3.8 \times 10^{15}$  Hz, can also be described by Eqn (23), which is universal for nonlinear systems, with the stationary solution (25). Evidently, different specimens of *trans*-PA may be characterised by different sets of the constants  $\varepsilon$ ,  $\kappa$ , and  $\beta$  in Eqn (23), so that the nature of the motion of the quasi-particles in these polymers may differ somewhat from that described above.

## V. Conclusion

It was shown above that the mechanism and rate of charge transfer in PA depend on the conformation, packing density, intramolecular dynamics, and lengths of the polymer chains in the undoped sample. In *cis*-PA, the neutral solitons are trapped in short sections of the *trans*-conformer. As a consequence of this, the probability of the intersoliton charge jump is exceptionally low and  $\sigma_{dc} \sim 10^{-11}$  S m<sup>-1</sup>. In the course of the *cis*–*trans* isomerisation, the length of the *trans*-chains increases, which leads to the ‘unfreezing’ of the mobility of some of the solitons. These quasi-particles acquire a charge and transport it along the chain up to the section where its tunnelling transfer to another soliton, moving along a neighbouring polymer chain, is most probable. As a result of this process, characterised by a fairly strong Raman interaction of the electron spins with the lattice phonons, a sharp increase in the electrical conductivity of the undoped PA actually occurs (up to  $\sigma_{dc} \sim 10^{-3}$  S m<sup>-1</sup>). It must be emphasised that the mobile solitons play an indirect role in the charge transfer in PA, so that the electron transport considered

may operate only in undoped and lightly doped *trans*-PA. On doping, the number of mobile and pinned paramagnetic centres diminishes and the dimensionality of the system increases, which alters the mechanism of the charge transfer.

The data obtained demonstrate the evident advantages of the two-millimetre EPR spectroscopy in the study of different *cis*- and *trans*-PA specimens, which make it possible to analyse more fully and correctly the magnetic and relaxation parameters of paramagnetic centres with different mobilities and to obtain information about the detailed characteristics of the molecular and spin dynamics in PA. Evidently this method can be used successfully also in the study of other organic polymeric semiconductors.

## References

1. J L Brédas, R Silbey (Eds) *Conjugated Polymers* (Dordrecht: Kluwer, 1991)
2. H Stubb, E Punkka, J Paloheimo *Mater. Sci. Eng.* **10** 85 (1993)
3. T E Scotheim (Ed.) *Handbook of Conducting Polymers* Vols 1, 2 (New York: Marcel Dekker, 1986)
4. R H Baughmann, S L Hsu, G P Pez, A J Signorelli *J. Chem. Phys.* **68** 5405 (1978)
5. C R Fincher, C-E Chen, A J Heeger, A G MacDiarmid, J B Hastings *Phys. Rev. Lett.* **48** 100 (1982)
6. W P Su, J R Schrieffer, A J Heeger *Phys. Rev. B, Condens. Matter* **22** 2209 (1980)
7. W Markowitsch, G Leising *Synth. Met.* **51** 25 (1992)
8. W Markowitsch, F Kuchar, K Seeger, in *Electronic Properties of Polymers and Related Compounds* (Eds H Kuzmany, M Mehring, S Roth) (Berlin: Springer, 1985) p. 78
9. H Thomann, L R Dalton, in *Handbook of Conducting Polymers* Vol. 2 (Ed. T E Scotheim) (New York: Marcel Dekker, 1986) p. 1157
10. A J Epstein, in *Handbook of Conducting Polymers* Vol. 2 (Ed. T E Scotheim) (New York: Marcel Dekker, 1986) p. 1041
11. S Kivelson *Phys. Rev. B, Condens. Matter* **25** 3798 (1982)
12. N F Mott, E A Davis *Electronic Processes in Non-Crystalline Materials* (Oxford: Clarendon Press, 1979)
13. Y Wada, J R Schrieffer *Phys. Rev. B, Condens. Matter* **18** 3897 (1978)
14. K Maki *Phys. Rev. B, Condens. Matter* **26** 2178; 2181 (1982)
15. A Terai, Y Ono *Synth. Met.* **55-57** 4672 (1993)
16. P Bernier, in *Handbook of Conducting Polymers* Vol. 2 (Ed. T E Scotheim) (New York: Marcel Dekker, 1986) p. 1099
17. T S Zhuravleva *Usp. Khim.* **56** 128 (1987) [*Russ. Chem. Rev.* **56** 69 (1987)]
18. I B Goldberg, H R Crowe, P R Newman, A J Heeger, A G MacDiarmid *J. Chem. Phys.* **70** 1132 (1979)
19. S A Brazovskii *Zh. Eksp. Teor. Fiz.* **78** 677 (1980)
20. A Grupp, P Höfer, H Kass, M Mehring, R Weizenhöfer, G Wegner, in *Electronic Properties of Conjugated Polymers* (Eds H Kuzmany, M Mehring, S Roth) (Berlin: Springer, 1987) p. 156
21. P Bernier, C Linaya, M Disi, I Sledz, I M Fabre, F Schue, L Giral *Polym. J.* **13** 201 (1981)
22. K Holczer, J P Boucher, F Devreux, M Nechtschein *Phys. Rev. B, Condens. Matter* **23** 1051 (1981)
23. A Bartl, J Fröhner, R Zuzok, S Roth *Synth. Met.* **51** 197 (1992)
24. F Rachdi, P Bernier in *Electronic Properties of Conjugated Polymers* (Eds H Kuzmany, M Mehring, S Roth) (Berlin: Springer, 1987) p. 160
25. G Leizing, H Kahlert, O Leitner in *Electronic Properties of Conjugated Polymers* (Eds H Kuzmany, M Mehring, S Roth) (Berlin: Springer, 1987) p. 56
26. K Mizoguchi, K Kume, S Masubuchi, H Shirakawa *Solid State Commun.* **59** 465 (1986)
27. K Mizoguchi, K Kume, S Masubuchi, H Shirakawa *Synth. Met.* **17** 405 (1987)
28. K Mizoguchi, S Komukai, T Tsukamoto, K Kume, M Suezaki, K Akagi, H Shirakawa *Synth. Met.* **28** D393 (1989)
29. Y Tomkiewicz, T D Schultz, H B Broom, T C Clarke, G B Street *Phys. Rev. Lett.* **43** 1532 (1979)
30. M Nechtschein, F Devreux, R G Green, T C Clarke, G B Street *Phys. Rev. Lett.* **44** 356 (1980)
31. Y W Park, A J Heeger, M A Drury, A G MacDiarmid *J. Chem. Phys.* **73** 946 (1980)
32. T C Clarke, J C Scott, in *Handbook of Conducting Polymers* Vol. 2 (Ed. T E Scotheim) (New York: Marcel Dekker, 1986) p. 1127
33. F Masin, G Gusman, R Deltour *Solid State Commun.* **40** 415 (1981)
34. M Ziliox, P Spegt, C Mathis, B Francois, G Weill *Solid State Commun.* **51** 393 (1984)
35. K Mizoguchi, K Kume, H Shirakawa *Solid State Commun.* **50** 213 (1984)
36. K Mizoguchi, F Shimizu, K Kume, S Masubuchi *Synth. Met.* **41** 185 (1991)
37. N S Shiren, Y Tomkiewicz, T G Kazyaka, A R Taranko, H Thomann, L Dalton, T C Clarke *Solid State Commun.* **44** 1157 (1982)
38. Y Tomkiewicz, N S Shiren, T D Schultz, H Thomann, L Dalton, A Zetti, G Gruner, T C Clarke *Mol. Cryst. Liq. Cryst.* **83** 1049 (1982)
39. N S Shiren, Y Tomkiewicz, H Thomann, L Dalton, T C Clarke *J. Phys. (France)* **44** C3-223 (1983)
40. J C W Chien, G E Wnek, F E Karasz, J M Warakowski, L C Dickinson, A J Heeger, A G MacDiarmid *Macromolecules* **15** 614 (1982)
41. O Ya Grinberg, A A Dubinskii, Ya S Lebedev *Usp. Khim.* **52** 1490 (1983) [*Russ. Chem. Rev.* **52** 850 (1983)]
42. V I Krinichnyi *Zh. Prikl. Spektrosk.* **52** 887 (1990) [*Appl. Magn. Reson.* **2** 29 (1991)]
43. V I Krinichnyi *2-mm Wave Band EPR Spectroscopy of Condensed Systems* (Boca Raton, FL: CRC Press, 1995)
44. V I Krinichnyi, A E Pelekh, Ya S Lebedev, L I Tkachenko, G I Kozub, A Barrat, L G Brunel, G B Robert *Appl. Magn. Reson.* **7** 459 (1994)
45. M Nechtschein, F Devreux, F Genoud, M Guglielmi, K Holczer *Phys. Rev. B, Condens. Matter* **27** 61 (1983)
46. V I Krinichnyi, A E Pelekh, L I Tkachenko, G I Kozub *Synth. Met.* **46** 13 (1992)
47. Ya S Lebedev, V I Muromtsev *EPR i Relaksatsiya Stabilizirovannykh Radikalov* (EPR and Relaxation of Stabilised Radicals) (Moscow: Khimiya, 1972) p. 255
48. M T Jones, H Thomann, H Kim, L R Dalton, B H Robinson, Y Tomkiewicz *J. Phys. (France)* **44** 455 (1983)
49. V F Traven' *Elektronnaya Struktura i Svoistva Organicheskikh Molekul* (Electronic Structure and Properties of Organic Molecules) (Moscow: Khimiya, 1989)
50. C P Pool *Electron Spin Resonance: A Comprehensive Treatise on Experimental Techniques* (New York: Wiley, 1983)
51. M Mehring, H Weber, W Müller, G Wegner *Solid State Commun.* **45** 1075 (1983)
52. N N Tikhomirova, V V Voevodskii *Opt. Spektrosk.* **7** 829 (1959)
53. A Carrington, A D MacLachlan *Introduction of Magnetic Resonance* (New York: Harper and Row, 1967) (Translated into Russian; Moscow: Mir, 1970)
54. V I Krinichnyi, A E Pelekh, A Yu Brezgunov, L I Tkachenko, G I Kozub *Mater. Sci.* **17** 25 (1991)
55. P D Krasicky, R H Silsbee, J C Scott *Phys. Rev. B, Condens. Matter* **25** 5607 (1981)
56. V I Krinichnyi, A E Pelekh, L I Tkachenko, G I Kozub *Synth. Met.* **46** 1 (1992)
57. E A Silin'sh, M V Kurik, V Chapek, in *Elektronnnye Protssesy v Organicheskikh Molekulyarnykh Kristallakh: Yavleniya Lokalizatsii i Polyarizatsii* (Electronic Processes in Organic Molecular Crystals: Localisation and Polarisation Phenomena) (Riga: Zinatne, 1988) p. 177
58. Yu S Kivshar, B A Malomed *Rev. Mod. Phys.* **61** 763 (1989)
59. A E Pelekh, V I Krinichnyi, A Yu Brezgunov, L I Tkachenko, G I Kozub *Vysokomol. Soedin.* **33** 1731 (1991)
60. A A Bugai *Fiz. Tverd. Tela* **4** 3027 (1962)
61. A A Al'tshuller, B M Kozyrev *Elektronnnye Paramagnitnyi Rezonans Soedinenii Elementov Promezhutochnykh Grupp* (Electron Paramagnetic Resonance of Compounds of Intermediate Group Elements) (Moscow: Nauka, 1972)
62. P R Gullis *J. Magn. Reson.* **21** 397 (1976)

63. S P Kurzin, B G Tarasov, N F Fatkullin, R M Aseeva *Vysokomol. Soedin., Ser. A* **24** 117 (1982)
64. K Mizoguchi *Makromol. Chem. Makromol. Symp.* **37** 53 (1990)
65. J C W Chien, M A Schen *Macromolecules* **19** 1042 (1986)
66. L A Blyumenfel'd, V V Voevodskii, A G Semenov *Primenenie Elektronogo Paramagnitnogo Rezonansa v Khimii* (Applications of Electron Paramagnetic Resonance in Chemistry) (Novosibirsk: Izd. Sib. Otd. Akad. Nauk SSSR, 1962)
67. A Abragam *Principles of Nuclear Magnetism* (London: Oxford University Press, 1961)
68. M A Butler, L R Walker, Z G Soos *J. Chem. Phys.* **64** 3592 (1976)
69. G Paasch *Synth. Met.* **51** 7 (1992)
70. M El Kadiri, J P Parneix, in *Electronic Properties of Conjugated Polymers* (Eds H Kuzmany, M Mehring, S Roth) (Berlin: Springer, 1987) p. 183
71. P Kuivalainen, H Stubb, H Isotalo, L Yli-Lahti, C Holmström *Phys. Rev. B, Condens. Matter* **31** 7900 (1985)
72. A J Epstein, H Rommelmann, M A Druy, A J Heeger, A G MacDiarmid *Solid State Commun.* **38** 683 (1981)
73. B R Weinberger, J Kaufer, A J Heeger, A Pron, A G MacDiarmid *Phys. Rev. B, Condens. Matter* **20** 223 (1979)
74. V V Mank, N I Lebovka *Spektroskopiya Yadernogo Magnitnogo Rezonansa Vody v Geterogennykh Sistemakh* (Nuclear Magnetic Resonance Spectroscopy of Water in Heterogeneous Systems) (Kiev: Naukova Dumka, 1988)
75. G M Bartenev, S Ya Frenkel' *Fizika Polimerov* (The Physics of Polymers) (Leningrad: Khimiya, 1990)
76. Yu S Kivshar, B A Malomed *Rev. Mod. Phys.* **61** 763 (1989)